

Searching for a preferred direction with Union2.1 data

Xiaofeng Yang^{1,2,3*}, F. Y. Wang^{1,2†}, Zhe Chu⁴

¹ School of Astronomy and Space Science, Nanjing University, Nanjing, 210093, China

² Key Laboratory of Modern Astronomy and Astrophysics (Nanjing University), Ministry of Education, Nanjing 210093, China

³ State Key Laboratory of Frontiers in Theoretical Physics, Institute of Theoretical Physics, Chinese Academy of Sciences, Beijing, 100190, China

⁴ Key Laboratory for Research in Galaxies and Cosmology, Shanghai Astronomical Observatory, Chinese Academy of Sciences, Nandan Road 80, Shanghai, 200030, China

17 February 2020

ABSTRACT

A cosmological preferred direction was reported from the type Ia supernovae (SNe Ia) data in recent years. We use the Union2.1 data to give a simple classification of such studies for the first time. Because the maximum anisotropic direction is independent of isotropic dark energy models, we adopt two cosmological models (Λ CDM, w CDM) for the hemisphere comparison analysis and Λ CDM model for dipole fit approach. In hemisphere comparison method, the matter density and the equation of state of dark energy are adopted as the diagnostic qualities in the Λ CDM model and w CDM model, respectively. In dipole fit approach, we fit the fluctuation of distance modulus. We find that there is a null signal for the hemisphere comparison method, while a preferred direction ($b = -14.3^\circ \pm 10.1^\circ, l = 307.1^\circ \pm 16.2^\circ$) for the dipole fit method. This result indicates that the dipole fit is more sensitive than the hemisphere comparison method.

Key words: cosmology: theory - dark energy, Type Ia supernovae

1 INTRODUCTION

Einstein’s general relativity and the cosmological principle are the two key foundations in modern cosmology. Cosmologists usually assumed that the general relativity is the perfect law of gravity from small to large scales, which has been tested by many tests in solar system and a few cosmological tests (e.g.(Zhang et al. 2007)). The cosmological principle (Weinberg 2008) assumes that the universe is homogeneous and isotropic on a sufficiently large scale. In practice, the homogeneity and isotropy are confirmed by a variety of cosmological observations, such as cosmic microwave background radiation (CMBR) (Hinshaw et al. 2013), the secondary effect of CMB (Zhang & Stebbins 2011), galaxy pairs (Marinoni et al. 2012; Wang & Dai 2013) and the large scale structure (LSS) (Sebastian et al. 2011). So far there is no any conclusive evidence for an anisotropic cosmological model.

However, a possible challenge to the cosmological principle was reported in recent years. Schwarz & Weinhorst (2007) claimed that a statistically significant anisotropy of the Hubble diagram was found at 2σ level at $z < 0.2$ by using SNe Ia data. SNe Ia data has been examined previously to test the isotropy of the universe (Kolatt & Lahav 2001; Bonvin et al. 2006;

Gordon et al. 2007; Schwarz & Weinhorst 2007). For comparison, we can divide the previous studies into two approaches as follows. (i) Local Universe Constraint is defined as searching for preferred direction work with low redshift astronomical probes (e.g.(Colin et al. 2011; Kalus et al. 2012)). (ii) Non-local Universe Constraint is defined as the study with intermediate and high redshift data (e.g.(Antonioni & Perivolaropoulos 2010; Cai & Tuo 2012)), which includes the redshift tomography analysis (dividing full sample into different redshift bins).

Since there is no well accepted upper limit value of redshift about how large the local universe is currently, we simply choose $z_{local} \leq 0.2$ in our classification. It is obvious that if a preferred direction or any other kind of anisotropy really exists, the physical origins may be different between local and non-local universe. Various local effect can lead to anisotropy in local universe, such as the bulk flow towards the Shapley supercluster (Colin et al. 2011). Thus, the explanation of local universe anisotropy is complicate and subtle. But if the non-local universe anisotropy was confirmed by observation, the standard cosmological model (Λ CDM) based on cosmological principle must be modified. So there are two merits of our classification. First, it provides the difference of the probing scale. Second, it implicates the different theoretical origins. At the same time, one can easily take the study by model-independent manner in local universe constraint (Kalus et al. 2012) and by model-dependent way in non-local universe constraint

* E-mail:xfyang@nju.edu.cn

† E-mail:fayinwang@nju.edu.cn

(Cai & Tuo 2012). In previous works, there are serious differences and disagreements among the studies on the possible cosmological anisotropy. Some works found no statistically significant evidence for anisotropy using the SNe Ia data (Tomita 2001; Blomqvist 2008; Gupta et al. 2008, 2010; Blomqvist 2010). However, many studies found that there is a statistically significant anisotropy (Schwarz & Weinhorst 2007; Cooke & Lynden 2010; Colin et al. 2011) or a cosmological preferred direction (Antoniu & Perivolaropoulos 2010; Cai & Tuo 2012; Mariano & Perivolaropoulos 2012; Cai et al. 2013; Zhao et al. 2013). A few works either gave no distinct results (Cooray et al. 2010; Campanelli et al. 2011) or argued that the anisotropic result of local universe constraint is not contradiction to the Λ CDM model (Kalus et al. 2012).

In this work, we search for a cosmological preferred direction from the latest Union2.1 data for the first time. For the anisotropic analysis, we adopt two typical and sophisticated approaches which are hemisphere comparison (Antoniu & Perivolaropoulos 2010) and dipole fit (Mariano & Perivolaropoulos 2012). Since the preferred direction is almost independent of isotropic dark energy models (Cai & Tuo 2012), we choose two simple cosmological models, Λ CDM and w CDM for the hemisphere comparison approach, and Λ CDM for the dipole fit. In the first approach, we use the matter density and the equation of state of dark energy as the diagnostic qualities in the Λ CDM and w CDM, respectively. In the second method, we employ distance modulus as the diagnostic quality in Λ CDM model.

The paper is organized as follows. We present the Union2.1 data and the two methods in section 2. Section 3 gives the numerical results. We compare and discuss our results with other works in section 4. Section 5 is a brief summary.

2 THE DATA AND METHODS

2.1 The Union2.1 data and preliminary formulae

SNe Ia are important probes of the evolution of the universe. In this work, we use the Union2.1 sample which is a compilation consisting of 580 SNe Ia. The redshift range is from 0.015 to 1.414 (Suzuki et al. 2012). Comparing to the Union2 data, the updated Union2.1 data consists other 23 SNe Ia. Here we get the directions of Union2 data in the equatorial coordinates (right ascension and declination) to each SN Ia from Blomqvist et al. (2010). We get the directions of additional 23 datapoints from NED website¹. We also use the Union2.1 table from the SCP website², which includes each SN Ia's name, redshift, distance modulus and uncertainties. We translated the equatorial coordinates of SNe Ia to galactic coordinates (l, b) in the galactic systems (Smith 1989).

In Figure.1, we show the angular distributions of the Union 2.1 datapoints in galactic coordinates. The color represents the value of redshift according to the legend on the right. The figures are viewed above the north galactic equator and south galactic equator in the left panel and right

panel, respectively. For avoiding confusion, we do't show Union2 data and additional 23 data on the same sphere. We show Union2 data in top panels and additional 23 data in bottom panels, respectively. Some of datapoints are nearly overlap in different redshift because of the similar angular direction. It is obvious that the distribution of additional 23 datapoints are slightly more isotropic than the distribution of Union2 data.

We study the SNe Ia data in the classical way by applying the maximum likelihood method. In a flat FLRW cosmological model, the luminosity distance is

$$D_L(z) = (1+z) \int_0^z \frac{dz'}{E(z')}. \quad (1)$$

In the flat Λ CDM model, $E(z)$ can be parameterized by

$$E^2(z) = \Omega_{m0}(1+z)^3 + (1-\Omega_{m0}), \quad (2)$$

where Ω_{m0} is the matter density. For the w CDM model, $E(z)$ is

$$E^2(z) = \Omega_{m0}(1+z)^3 + (1-\Omega_{m0})(1+z)^{3+3w}, \quad (3)$$

where w is the equation of state of dark energy.

We use the distance modulus of SN Ia data by minimizing the χ^2 . The χ^2 for SNe Ia is obtained by comparing theoretical distance modulus

$$\mu_{th}(z) = 5 \log_{10}(D_L(z)) + \mu_0, \quad (4)$$

here,

$$\mu_0 = 42.38 - 5 \log_{10} h \quad (5)$$

is a nuisance parameter. The theoretical model parameter (Ω_{m0} or w) is determined by minimizing the value of χ^2 with observed μ_{obs} of SNe Ia:

$$\chi_{\text{SN}}^2(\Omega_{m0}, \mu_0) = \sum_{i=1}^{580} \frac{(\mu_{obs}(z_i) - \mu_{th}(\Omega_{m0}, \mu_0, z_i))^2}{\sigma_{\mu}^2(z_i)}. \quad (6)$$

Since the nuisance parameter μ_0 is independent of the dataset, we can expand χ_{SN}^2 with respect to μ_0 (Nesseris & Perivolaropoulos 2005):

$$\chi_{\text{SN}}^2 = A - 2\mu_0 B + \mu_0^2 C, \quad (7)$$

here

$$A = \sum_{i=1}^{580} \frac{(\mu_{obs}(z_i) - \mu_{th}(z_i, \mu_0 = 0))^2}{\sigma_{\mu}^2(z_i)},$$

$$B = \sum_{i=1}^{580} \frac{\mu_{obs}(z_i) - \mu_{th}(z_i, \mu_0 = 0)}{\sigma_{\mu}^2(z_i)},$$

$$C = \sum_{i=1}^{580} \frac{1}{\sigma_{\mu}^2(z_i)}.$$

The value of Eq. (7) is minimum for $\mu_0 = B/C$ at

$$\tilde{\chi}_{\text{SN}}^2 = \chi_{\text{SN},\text{min}}^2 = A - B^2/C, \quad (8)$$

which is not rely on μ_0 .

2.2 The hemisphere comparison approach

Currently, it is not easy to find the angular dependence of anisotropy at small scale with significant confidence level

¹ <http://ned.ipac.caltech.edu>

² <http://supernova.lbl.gov>

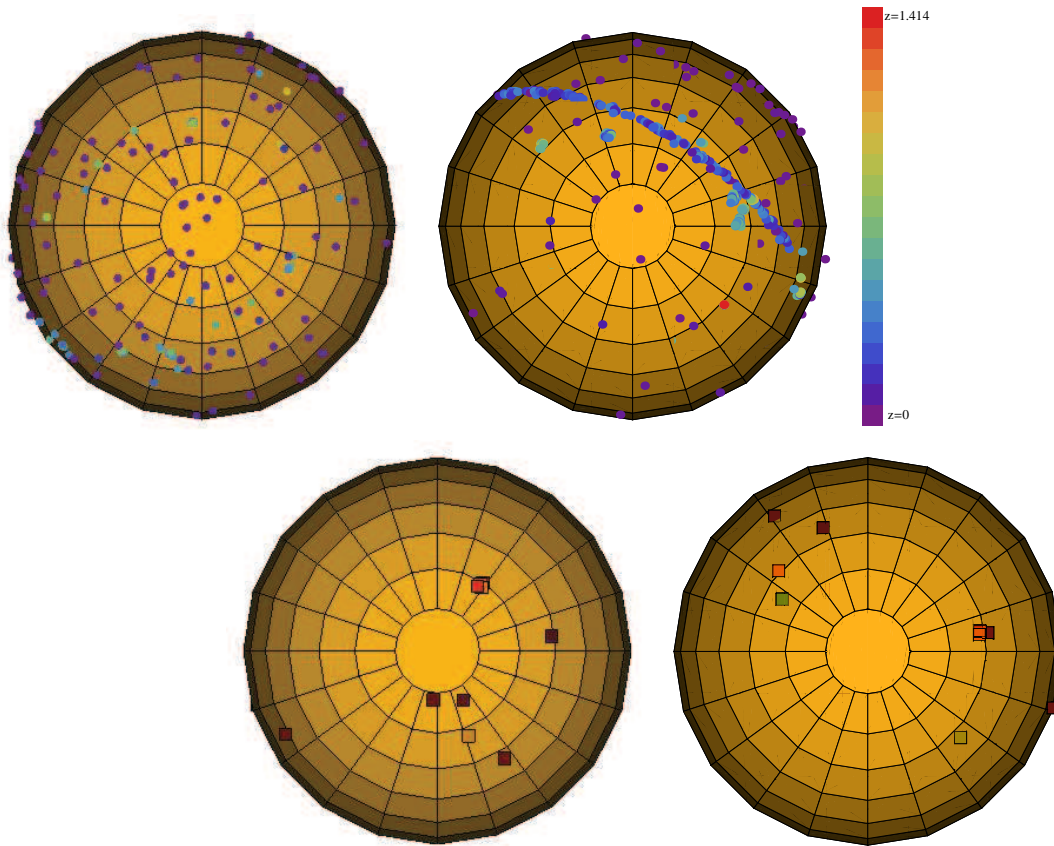


Figure 1. (color online) The Union2 data (up panels) and additional 23 data (bottom panels) in galactic coordinates. They are shown with viewpoint above the north galactic equator and south galactic equator in the left panel and right panel, respectively. The color of each point corresponds to the redshift of each SN Ia.

using SNe Ia. The reason is that the number density of SNe Ia is relatively low, particular in the tomography analysis. Thus, we firstly employ the hemisphere comparison for searching the largest possible anisotropy in the largest scale of $\pi/2$. An early similar research has been done to a CMB sky map analysis (Eriksen et al. 2004). The subsequent studies found one of the several anomalies in the WMAP data (e.g. Copi et al. 2007). The hemisphere comparison method was firstly proposed for searching largest possible anisotropy with SNe Ia by Schwarz & Weinhorst (2007). It was further developed and used for finding the possibly preferred direction (Antoniou & Perivolaropoulos 2010; Cai & Tuo 2012).

In recent works, different cosmological parameters are chosen as the diagnostic qualities, such as Ω_{m0} (Antoniou & Perivolaropoulos 2010), q_0 (Cai & Tuo 2012) and H_0 (Kalus et al. 2012). Since the preferred direction is weakly depended on dark energy models (Cai & Tuo 2012), we simply consider two cosmological models, such as Λ CDM and w CDM models. We also adopt Ω_{m0} and w for Λ CDM and w CDM as the diagnostic qualities, respectively. It could be convenient to compare previous results (Antoniou & Perivolaropoulos 2010) with ours.

We review the procedure of hemisphere comparison method in short (Antoniou & Perivolaropoulos 2010). (i) Generate a random direction with the same probability in unit sphere. (ii) Divide the dataset into two subsets according to the sign of the product between the vector generated

in the step (i) and the unit vector describing the direction of each SN Ia in the dataset. We can split the data in two opposite hemispheres, denoted by up and down. (iii) Calculate the best fit value of cosmological parameter on each hemisphere. (iv) Repeat a large times from step (i) to step (iii), and search the maximum normalized difference for the full data, thus one can get the preferred direction of maximum anisotropy.

One can get more details of this method from the two references (Antoniou & Perivolaropoulos 2010; Cai & Tuo 2012). Here, we just describe the third step of this method, which estimates the best parameter in each hemisphere. The subscripts u and d represent the best parameter fitting value in the ‘up’ and ‘down’ hemispheres, respectively. For estimating Ω_{m0} in Λ CDM model, we can define (Antoniou & Perivolaropoulos 2010)

$$\delta = \frac{\Delta\Omega_{m0}}{\Omega_{m0}} = \frac{\Omega_{m0,u} - \Omega_{m0,d}}{(\Omega_{m0,u} + \Omega_{m0,d})/2}. \quad (9)$$

For fitting w in the w CDM model, we define the relative anisotropic level with the equation of state of dark energy as

$$\delta' = \frac{\Delta w}{\bar{w}} = \frac{w_u - w_d}{(w_u + w_d)/2}, \quad (10)$$

where w_u and w_d are the best fitting equation of state in the ‘up’ and ‘down’ hemispheres, respectively. The number

of random axes should be more than the number of SNe Ia on each hemisphere. For Union2.1 sample, the number of data points per hemisphere is approximate 290, we choose 400 axes in this works. Since the hemisphere comparison approach is not pretty fine and sensitive enough to particular types of anisotropy (Mariano & Perivolaropoulos 2012), it is just a rough estimation for global property. We only implement the non-local universe constraint without redshift tomography if there is no any anisotropic signal in global constraint with the full sample in all redshift ranges.

2.3 The dipole fit approach

Dipole anisotropic fit method has been used for searching the anisotropy of fine structure constant with quasars on cosmological scale. Mariano & Perivolaropoulos (2012) firstly applied this method to anisotropic study using SNe Ia (Mariano & Perivolaropoulos 2012). The main steps of the dipole fit method are shown as follows:

- Convert the equatorial coordinates of SNe Ia to galactic coordinates.
- Give the Cartesian coordinates of unit vectors \hat{n}_i corresponding each SN Ia with galactic coordinates (l, b) . So, we obtain

$$\hat{n}_i = \cos(b_i) \cos(l_i) \hat{i} + \cos(b_i) \sin(l_i) \hat{j} + \sin(b_i) \hat{k}. \quad (11)$$

- Define the angular distribution model with dipole and monopole

$$\left(\frac{\Delta\mu}{\bar{\mu}}\right) = d \cos\theta + m, \quad (12)$$

where μ is distance modulus, m and d denote the monopole and dipole magnitude, respectively, $\cos\theta$ is the angle with the dipole axis defined by the vector

$$\vec{D} \equiv c_1 \hat{i} + c_2 \hat{j} + c_3 \hat{k}. \quad (13)$$

So

$$\hat{n}_i \cdot \vec{D} = d \cos\theta_i. \quad (14)$$

Then, we can fit the SNe Ia data to a dipole anisotropy model (12) using the maximum likelihood method by minimizing

$$\chi^2(\vec{D}, m) = \sum_{i=1}^{580} \frac{\left[\left(\frac{\Delta\mu}{\bar{\mu}}\right)_i - d \cos\theta_i - m\right]^2}{\sigma_i^2}. \quad (15)$$

- At last, we can obtain the magnitude and direction of the best fit dipole in galactic coordinates from the best fit c_i coordinates (e.g. $d = \sqrt{c_1^2 + c_2^2 + c_3^2}$). The corresponding 1σ errors are obtained using the covariance matrix approach.

3 THE RESULTS

3.1 Results of hemisphere comparison method

We apply the hemisphere comparison method using the latest Union2.1 dataset. Generally, one can expect that we should get the similar results with recent works from Union2 sample (Antoniou & Perivolaropoulos 2010; Cai & Tuo 2012). It is surprised that we get different results compared with previous works.

Table 1 shows our numerical results with the Union2.1 dataset, which could be clearly compared with previous results shown in the second row (Antoniou & Perivolaropoulos 2010). The 1σ error is propagated from the uncertainties of the SNe Ia distance moduli. The superscript *Real* and *Sim* denote the maximum anisotropic values which are obtained from real SNe Ia dataset and a typical isotropic simulated dataset, respectively. The simulated isotropic dataset has been constructed by replacing each real data distance modulus to a random number from the normal distribution with mean and standard deviation obtained by the best fitting value of $\mu_{th}(z_i)$ and by uncertainties of the corresponding real data point, respectively. Comparing to the result derived from Union2 dataset, it is clear that the maximum anisotropy level is 0.31 ± 0.05 for the Union2.1 dataset. However, the value is 0.35 ± 0.05 for simulation data, which is larger than the one of real data. In this calculation, the same parameter and cosmology model (Λ CDM) are used for the two different datasets.

The maximum anisotropic value will convergence in calculations with real data by enlarging the random selected axes, whereas it's precise value will be fluctuated in repeated estimations with simulated data for random selected effect. In w CDM model calculation, the value of Eq.(10) is 0.27 ± 0.07 and 0.37 ± 0.07 in real data and simulated data, respectively. The value of real data is smaller than the one in Λ CDM fitting (0.31 ± 0.05) for different cosmological parameter and model. The value (0.37 ± 0.07) in this simulation dataset is still larger than the one in real data (0.27 ± 0.07).

Although our results show that the maximum anisotropy level is lower than simulation isotropic dataset from Union2.1 dataset, we still process the same numerical experiments as shown in the Antoniou & Perivolaropoulos (2010). The purpose is to answer whether the maximum anisotropy level for real data is higher or lower than statistical isotropy. This kind of numerical experiments is not intend to identify the maximum anisotropic direction in standard 400 axes searching procedure. We only want to compare the real data with the isotropic simulation data. It is important to repeat the comparison many times (40 in our case) for acceptable statistics. Because of the limitations of searching time, we adopt 10 axes for employing fast-speed Monte Carlo experiments (Antoniou & Perivolaropoulos 2010). This numerical experiment is important because of more fluctuated values with maximum anisotropy level in the simulation data.

From a set of numerical experiments, we get different results from Union2.1 dataset comparing with Union2 dataset in Table 2. The *Real* or *Sim* denotes the number of cases which maximum anisotropic value of real data is larger or smaller than that of simulated data, respectively. For Union2 dataset, there is about 1/3 of the numerical experiments with $\delta_{max}^{Sim} > \delta_{max}^{Real}$, which means that the anisotropy level was larger than the one of the isotropic simulation data (Antoniou & Perivolaropoulos 2010). However, we find that the possibility of real data and simulation data which have a larger maximum anisotropic value is nearly equal. The results in Table 2 are not consistent with the work of Antoniou & Perivolaropoulos (2010). In order to test the dependence on the number of axes, we increase the random axes from 10 to 50. As shown in Table 2, our conclusion is unchanged.

Since there is no anisotropic signal in global constraint

Table 1. The value of maximum anisotropy for Union2.1 dataset and isotropic simulation dataset. The second row is the value calculated from Union2 dataset (Antoniou & Perivolaropoulos 2010).

Model(Sample)	Diagnostic	δ_{max}^{Real}	δ_{max}^{Sim}
Λ CDM(Union2)	Ω_{m0}	0.43 ± 0.06	0.36 ± 0.06
Λ CDM(Union2.1)	Ω_{m0}	0.31 ± 0.05	0.35 ± 0.05
w CDM (Union2.1)	w	0.27 ± 0.07	0.37 ± 0.07

Table 2. The results of 40 times numerical experiments for the value of maximum anisotropy with Union2.1 dataset and isotropic simulation datasets. The second row is the result from Union2 dataset (Antoniou & Perivolaropoulos 2010). The Real or Sim denotes the number of cases which maximum anisotropic value of real data is larger or smaller than that of simulated data, respectively.

Model(Sample)	Axes×All times	Real	Sim
Λ CDM(Union2)	10×40	26	14
Λ CDM(Union2.1)	10×40	19	21
	20×40	17	23
	30×40	20	20
	40×40	22	18
	50×40	18	22
w CDM (Union2.1)	10×40	18	22
	20×40	19	21
	30×40	17	23
	40×40	21	19
	50×40	20	20

with full Union2.1 data, we will not apply the redshift tomography analysis in this work. We use tomography analysis in next subsection which implements a more sensitive searching approach.

3.2 Results of dipole fit method

We study the latest Union2.1 dataset using the dipole fit method, which includes non-local universe constraint and tomography constraint. First, we report the result of non-local universe constraint with full Union2.1 data. Then, we will show the local universe constraint and tomography results.

We find the direction of the dark energy dipole with full data

$$b = -14.3^\circ \pm 10.1^\circ, l = 307.1^\circ \pm 16.2^\circ. \quad (16)$$

The values of the dipole and monopole magnitudes are

$$d_{Union2.1} = (1.2 \pm 0.5) \times 10^{-3}, \quad (17)$$

$$m_{Union2.1} = (1.9 \pm 2.1) \times 10^{-4}. \quad (18)$$

The statistical significance of the dark energy dipole is about at the 2σ level. The direction of Union2 dipole is ($b = -15.1^\circ \pm 11.5^\circ, l = 309.4^\circ \pm 18.0^\circ$)(Mariano & Perivolaropoulos 2012), and the dipole and monopole magnitudes are

$$d_{Union2} = (1.3 \pm 0.6) \times 10^{-3}, \quad (19)$$

$$m_{Union2} = (2.0 \pm 2.2) \times 10^{-4}. \quad (20)$$

The statistical significance of the dark energy dipole is also at the 2σ level using Union2, thus, our results are consistent with Mariano & Perivolaropoulos 2012.

According to the dipole fit approach (Mariano & Perivolaropoulos 2012), we determine the likelihood of the observed dark energy dipole magnitude with performing a Monte Carlo simulation consisting of 10^4 Union2.1 datasets constructed under the assumption of isotropic Λ CDM. The distance modulus of point i is defined as

$$\mu_{MC}(z_i) = g(\bar{\mu}(z_i), \sigma_i), \quad (21)$$

where g is the Gaussian random selection function (Mariano & Perivolaropoulos 2012), and $\bar{\mu}(z_i)$ is the best fit distance modulus of the Union2.1 full data in Λ CDM model at redshift z_i . It is convenient to construct $\left(\frac{\Delta\mu(z_i)}{\bar{\mu}(z_i)}\right)_{MC}$ for each Monte Carlo dataset and search its best fit dipole direction and magnitude. In Figure. 2 we show the probability distribution of the dark energy dipole magnitude along with the observed dipole magnitude represented by an arrow. As expected from Equation. (17) merely 4.55% of the simulations had a dark energy dipole magnitude bigger than the value in real dataset. The result is consistent with Equation. (17) which indicates that the statistical significance of the dark energy dipole is about 2σ . For the number of Monte Carlo simulation, previous work proved that 10^4 adopted as the number of simulated datasets is enough to obtain a significant results (Mariano & Perivolaropoulos 2012).

We also take the redshift tomography analysis for indicating these effects in different redshift ranges. We adopt two subsample allocations similar as previous work based on Union2 (Mariano & Perivolaropoulos 2012), one is partitioning full sample with three redshift bins and the other is changing the redshift upper limit. In the first method, we divide full dataset into three redshift bins which have nearly the same number of SNe Ia. Then we perform the similar works as above in each bin and compare the results of each bin with respect to the quality of data with errors, the dipole magnitudes and the dipole directions. For the second method, we set first and second subsample with an redshift upper limit consisting of about a half of the full datapoints. Then we enlarge the redshift upper limit properly so that the largest subsample almost includes full dataset. We study each subsample of the six cumulative dataset parts with the same procedure as above.

Table 3 shows our results in different redshift ranges with each subsample of Union2.1, which includes our above non-local universe constraint in the second line. It also shows the deviled method of redshift bins and the datapoints number of each redshift bin. In 2nd to 5th columns, the results in brackets are from Union2 data (Mariano & Perivolaropoulos 2012). In the last column, the number in and out brackets is the datapoints of Union2 and Union2.1, respectively. There is no additional datapoint from Union2 to Union2.1 in the redshift $0.14 < z \leq 0.43$. In each redshift bin or range, we show the corresponding best fit monopole magnitude, the dipole magnitude and the direction of the best fit dipole in galactic coordinates. The uncertainties shown in Table 3 are calculated via the covariance matrix approach. We have checked and confirmed that they are consistent with the corresponding 1σ errors calculated from the Monte Carlo simulations. All the results we reported here in the Table 3 are consistent with the results from Union2 (Mariano & Perivolaropoulos 2012). We also find

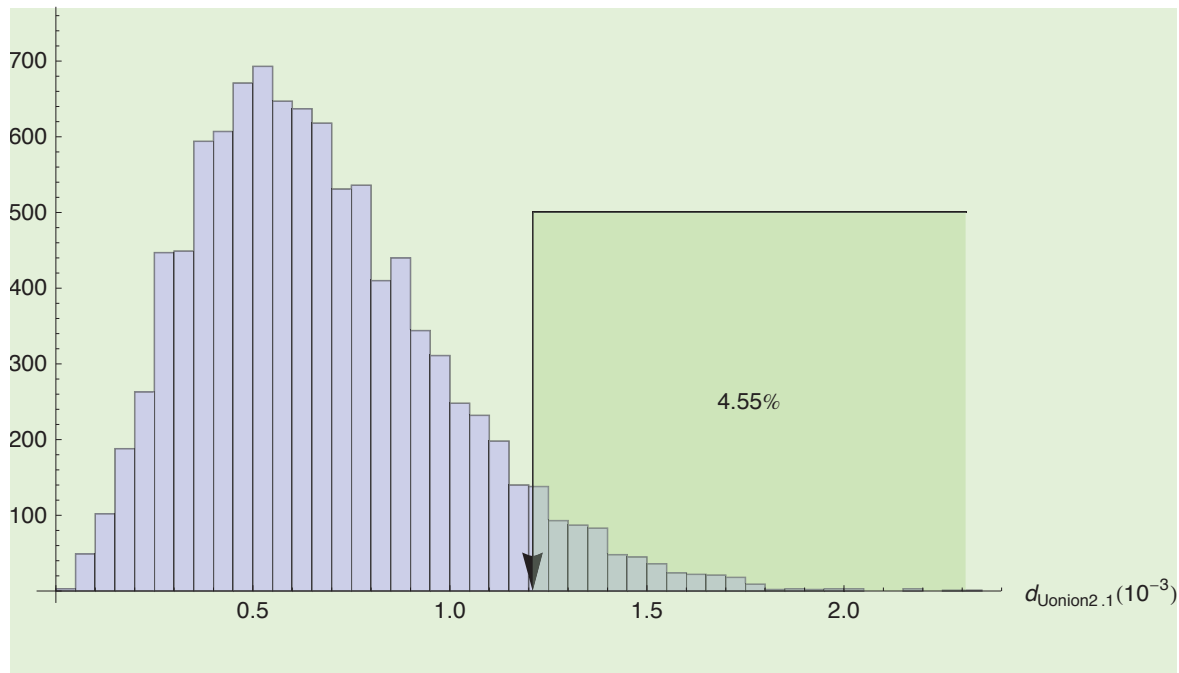


Figure 2. (color online). Histogram of distribution indicates the dark Energy dipole magnitudes from the Monte Carlo simulation. The arrow position is the observed best fit value. The deeper green region shows fraction of the Monte Carlo datasets that give a dipole magnitude larger than the observed best fit one.

that the “best” redshift bin with the smallest errors for the Union2.1 data is the lowest redshift bin ($0.015 < z \leq 0.14$), which is also similar to previous work from Union2 (Mariano & Perivolaropoulos 2012).

4 DISCUSSION

If a preferred direction or any other anisotropy could be really confirmed at high significant level, particular in non-local universe ($z > 0.2$), we should abandon cosmological principle and study the anisotropic cosmological models, e.g. vector field model, Bianchi type I model or extended topological quintessence model (Mariano & Perivolaropoulos 2012). A comprehensive introduction of various observational probes on the preferred axis could be found in the paper (Perivolaropoulos 2011). So far, the largest anisotropic value (> 0.7) is given by Cai & Tuo (2010)’s work from Union2 data, which adopted the deceleration parameter q_0 for estimation via hemisphere comparison method. However, in all of previous works, the significance of the violation to isotropic assumption of cosmological principle are not high. In fact, most of them are no more than 2σ confidence level. Although people have proved that the significance could be improved by correlations with other preferred axes from different observations (Antoniou & Perivolaropoulos 2010), none of them has been confirmed or has acceptable fundamental physical theory. Since there are tensions in cosmological constraints with different observations, maybe it need more works on this issue with different probes.

There are merely adding 23 data points in this paper, thus it is not reasonable that we get the different results compared with previous works based on Union2. Interesting, we have the different results by the hemisphere

comparison method but obtain the same results by the dipole fit method. There are three potential reasons for such differences. The first is the possible tension between Union2 and Union2.1. Second, the different space distribution is another factor. The third reason is the different method’s sensitivity. For the data tension, recently, some other independent works focused on constraining the dark energy model point out the tension in datasets between Union2 and Union2.1 (e.g.(Zhang et al. 2013)). For the different distribution, we show that the distribution of Union2.1 dataset is slightly better-distributed than the one of Union2, this hint could be found in Figure 1. However, Kalus et al.(2012) argued that the non-uniform distribution has no significant impact on such anisotropic estimation. Since their work is just local universe constraint whereas our and the two other hemisphere comparison works (Antoniou & Perivolaropoulos 2010; Cai & Tuo 2012) are non-local universe constraints, the detailed analysis of the different anisotropic searching results by hemisphere comparison method and other methods beyond the scope of this work. The third aspect may be the main point, which is caused by that the dipole fit method is more sensitive and effective than hemisphere comparison method (Mariano & Perivolaropoulos 2012). Generally, our results confirm this idea with Union2.1 data. On the other hand, although hemisphere comparison method is neither precise nor perfect, it is really a model-independent approach. Since we should define the angular distribution model as a fiducial model in dipole fit method, it is much more model-dependent than hemisphere comparison method. This situation is similar to the studies on dark energy reconstruction. Many dark energy parameterizations could enhance the precision of dark energy parameters constraint, but

Table 3. The results of dipole fit approach including non-local, local constraints and tomography analysis. In the 2nd to 5th columns, we show the monopole magnitude, dipole magnitude and direction from the estimation with Union2.1 (Union2) data in different redshift ranges (1st column). Expect for the last column, the results in brackets are the calculations from Union2 data (Mariano & Perivolaropoulos 2012) for comparison. In the last column, the number in and out brackets represents the datapoints of Union2 and Union2.1, respectively. There are the same datapoints between Union2.1 and Union2 in the redshift $0.14 < z \leq 0.43$.

	$\frac{m_{U2.1}(m_{U2})}{10^{-4}}$	$\frac{d_{U2.1}(d_{U2})}{10^{-3}}$	$b_{d_{U2.1}}(b_{d_{U2}})$	$l_{d_{U2.1}}(l_{d_{U2}})$	U2.1(U2)
$0.015 \leq z \leq 1.414$	$1.9 \pm 2.1(2.0 \pm 2.2)$	$1.2 \pm 0.5(1.3 \pm 0.6)$	$-14.3 \pm 10.1(-15.1 \pm 11.5)$	$307.1 \pm 16.2(309.4 \pm 18.0)$	580(577)
$0.015 < z \leq 0.14$	$2.5 \pm 3.1(2.6 \pm 3.4)$	$1.5 \pm 0.7(1.7 \pm 0.8)$	$-9.8 \pm 14.6(-10.1 \pm 15.1)$	$304.3 \pm 21.4(308.8 \pm 22.8)$	193(184)
$0.14 < z \leq 0.43$	2.6 ± 5.6	1.2 ± 1.9	-10.7 ± 28.7	291.4 ± 37.2	186(186)
$0.43 < z \leq 1.414$	$0.6 \pm 3.7(0.7 \pm 4.3)$	$0.7 \pm 0.7(0.9 \pm 0.8)$	$-25.9 \pm 29.7(-25.1 \pm 30.6)$	$35.7 \pm 73.1(34.3 \pm 75.7)$	201(187)
$0.015 \leq z \leq 0.23$	$3.2 \pm 2.7(3.3 \pm 2.9)$	$1.6 \pm 0.6(1.8 \pm 0.7)$	$-7.8 \pm 11.9(-8.5 \pm 12.4)$	$300.3 \pm 16.1(302.2 \pm 16.6)$	248(239)
$0.015 \leq z \leq 0.31$	$3.5 \pm 2.7(3.8 \pm 2.9)$	$1.7 \pm 0.6(1.9 \pm 0.7)$	$-6.8 \pm 11.1(-7.6 \pm 11.6)$	$304.5 \pm 13.6(307.0 \pm 14.7)$	301(292)
$0.015 \leq z \leq 0.41$	$2.8 \pm 2.6(3.0 \pm 2.7)$	$1.6 \pm 0.6(1.8 \pm 0.7)$	$-13.8 \pm 9.7(-14.4 \pm 10.3)$	$301.5 \pm 13.5(303.6 \pm 14.4)$	361(352)
$0.015 \leq z \leq 0.51$	$2.1 \pm 2.5(2.2 \pm 2.6)$	$1.3 \pm 0.6(1.4 \pm 0.7)$	$-14.1 \pm 12.1(-14.9 \pm 12.7)$	$298.8 \pm 17.8(301.3 \pm 18.8)$	415(406)
$0.015 \leq z \leq 0.64$	$2.0 \pm 2.2(2.1 \pm 2.4)$	$1.3 \pm 0.5(1.4 \pm 0.6)$	$-15.5 \pm 10.7(-16.0 \pm 11.0)$	$302.4 \pm 16.1(305.3 \pm 16.9)$	474(464)
$0.015 \leq z \leq 0.89$	$1.8 \pm 2.1(2.2 \pm 2.3)$	$1.3 \pm 0.5(1.4 \pm 0.6)$	$-14.8 \pm 10.0(-15.6 \pm 10.4)$	$307.3 \pm 15.2(309.8 \pm 16.0)$	531(519)

the parameterizations also impose some bias on the exact evolution of dynamical dark energy. Correspondingly, if we adopt any specific angular distribution model in dipole fit method, such as the Equation.12 or the parameterization in Cai et al's work (Cai et al. 2013), it may affect the result of the potential unbiased anisotropy of the universe. We will investigate this interesting issue in future works. The high-redshift data, such as gamma-ray bursts will be included (Basilakos & Perivolaropoulos 2008; Wang, Qi & Dai 2011; Wang & Dai 2011).

5 SUMMARY

In this paper, we search for a preferred direction of acceleration using the Union2.1 SNe Ia sample. At the beginning of this paper we simply specify and classify previous searching works into two types according to their sample's redshift ranges. Many authors found that a maximum (minimum) expansion (acceleration) in a preferred direction by applying the hemisphere comparison method and dipole fit method to SNe Ia sample. We use the latest Union2.1 sample on this study for the first time. We adopt two cosmological models (Λ CDM, w CDM) for hemisphere comparison method and Λ CDM model for dipole fit. In hemisphere comparison approach, we use matter density and the equation of state of dark energy as the diagnostic qualities in Λ CDM and w CDM models, respectively. In dipole fit approach, we study the fluctuation of distance modulus and take the tomography analysis with different redshift ranges. Comparing with Union2, we find a null signal for cosmological preferred direction by hemisphere comparison method. But there is a preferred direction ($b = -14.3^\circ \pm 10.1^\circ, l = 307.1^\circ \pm 16.2^\circ$) by dipole fit approach. Our results confirm that the dipole fit method is more sensitive than the hemisphere comparison method for the searching of a cosmological preferred direction with SNe Ia.

ACKNOWLEDGMENTS

We thank the referee Prof. Perivolaropoulos very much for the detail and constructive suggestions which helped to improve the manuscript significantly. We have benefited from reading the publicly available codes of Antoniou &

Perivolaropoulos (2010) and Mariano & Perivolaropoulos (2012). Xiaofeng Yang gratefully acknowledges the collaborating, long visiting and open fund provided by State Key Laboratory of Theoretical Physics, Institute of Theoretical Physics, Chinese Academy of Sciences, where the last revision of this manuscript was completed in. This work is supported by the National Basic Research Program of China (973 Program, grant 2014CB845800) and the National Natural Science Foundation of China (grants 11373022, 11103007, and 11033002).

REFERENCES

- Antoniou, A., Perivolaropoulos, L., 2010, JCAP, 12, 012
 Basilakos S., Perivolaropoulos L., 2008, MNRAS, 391, 411
 Blomqvist. M., Mortsell. E., Nobili., S., 2008, JCAP, 06, 027
 Blomqvist. M., Enander. J., Mortsell. E., 2010, JCAP, 10, 018
 Bonvin, C., Durrer, R., Kunz, M., 2006, Phys. Rev. Lett., 96, 191302
 Cai, R. G., Tuo, Z. L., 2012, JCAP, 02, 004
 Cai, R. G., Ma, Y. Z., Tang, B., Tuo, Z. L., 2013, PRD, 87, 123522
 Cooke, R., Lynden, B., D., 2010, MNRAS, 401, 1409
 Cooray, A. R., Holz, D. E., Caldwell, R., 2010, JCAP, 11, 015
 Copi, C. J., Huterer, D., Schwarz, Z., Starkman, G. D., 2007, PRD, 75, 023507
 Colin, J., Mohayaee, R., Sarkar, S., Shafieloo, A. 2011, MNRAS, 414, 264
 Campanelli, L., Cea, P., Fogli, G. L., Marrone. A., 2011, PRD, 83, 103503
 Eriksen, H. K., Hansen, F. K., Banday. A. J., Gorski. K. M., Lilje. K. M., 2004, ApJ, 605, 14
 Gordon, C., Land, K. & Slosar, A., 2007, Phys. Rev. Lett., 99, 081301
 Gupta, S., Saini, T. D., Lskar, T., 2008, MNRAS, 388, 242
 Gupta, S., Saini, T. D. 2010, MNRAS, 407, 651
 Hinshaw, S. et al., 2013, ApJS, 208, 19
 Kalus. B., Schwarz, D. J., Seikel, M., Wiegand, A. 2012, A&A, 478, 719
 Kolatt, T. S. & Lahav, O., 2001, MNRAS, 323, 859.

- Mariano, A., Perivolaropoulos, L., 2012, PRD, 86, 083517
Marinoni, C., Bela, J., Buzzia, A., 2012, JCAP, 10, 036
Nesseris, S., & Perivolaropoulos, L., 2005, PRD, 72,123519
Perivolaropoulos, L., 2011, arXiv:astro-ph/1104.0539
Schwarz, D. J., & Weinhorst. B, 2007, A&A, 474, 719
Sebastian, T. G., Klypin. A., Primack. J., Romanowsky. R.
J. 2011, ApJ, 742, 1
Suzuki, N., et al. 2012, ApJ, 746, 85
Smith, D. P, 1989, Practical astronomy with your calculator, Cambridge University Press, Cambridge U.K.
Tomita, A., 2001, Progress in Theoretical Physics, 106, 929
Wang F. Y., Dai Z. G., 2011, A&A, 536, A96
Wang, F. Y., Dai, Z. G., 2013, MNRAS, 432, 3025.
Wang F. Y., Qi S., Dai Z. G., 2011, MNRAS, 415, 3423
Weinberg, S., 2008, Cosmology, Oxford University Press, Oxford U.K.
Zhao, W., Wu.P.X., Zhang.Y., 2013, IJMPD, 22, 1350060
Zhang, J., Li, Y., Zhang, X., 2013, EPJC, 73, 2280
Zhang, P., Liguori, M., Bean, R., Dodelson, S. 2007, Phys. Rev. Lett., 99, 141302
Zhang, P., Stebbins, A. 2011, Phys. Rev. Lett., 107,041301